Two distinct overstretched DNA structures revealed by single-molecule thermodynamics measurements

Xinghua Zhang[a,b,c], Hu Chen[b], Hongxia Fu[b], Patrick S. Doyle[a,d,1], and Jie Yan[a,b,c,e,1]

[a]BioSystems and Micromechanics (BioSyM), Singapore-MIT Alliance for Research and Technology, National University of Singapore, Singapore 117543; [b]Mechanobiology Institute, National University of Singapore, Singapore 117411; [c]Department of Physics, National University of Singapore, Singapore 117542; [d]Department of Chemical Engineering, Massachusetts Institute of Technology (MIT), 77 Massachusetts Avenue, Cambridge, MA 02139; and [e]Centre for Bioimaging Sciences, National University of Singapore, Singapore 117546

Double-stranded DNA is a dynamic molecule whose structure can change depending on conditions. While there is consensus in the literature about many structures DNA can have, the state of highly-stretched DNA is still not clear. Several groups have shown that DNA in the torsion-unconstrained B-form undergoes an "overstretching" transition at a stretching force of around 65 pN, which leads to approximately 1.7-fold elongation of the DNA contour length. Recent experiments have revealed that two distinct structural transitions are involved in the overstretching process: (*i*) a hysteretic "peeling" off one strand from its complementary strand, and (*ii*) a nonhysteretic transition that leads to an undetermined DNA structure. We report the first simultaneous determination of the entropy (ΔS) and enthalpy changes (ΔH) pertaining to these respective transitions. For the hysteretic peeling transition, we determined $\Delta S \sim 20$ cal/(K·mol) and $\Delta H \sim 7$ kcal/mol. In the case of the nonhysteretic transition, $\Delta S \sim -3$ cal/(K·mol) and $\Delta H \sim 1$ kcal/mol. Furthermore, the response of the transition force to salt concentration implies that the two DNA strands are spatially separated after the hysteretic peeling transition. In contrast, the corresponding response after the nonhysteretic transition indicated that the strands remained in close proximity. The selection between the two transitions depends on DNA base-pair stability, and it can be illustrated by a multidimensional phase diagram. Our results provide important insights into the thermodynamics of DNA overstretching and conformational structures of overstretched DNA that may play an important role in vivo.

entropy and enthalpy | S-DNA | ssDNA | B-to-S transition

DNA can exist as a single-stranded polymer or a double-stranded helical structures. In cells, DNA primarily exists in the stable B-form (B-DNA), which contains two strands that are associated by Watson-Crick base-pairing interactions, and are stabilized by stacking interaction between adjacent base pairs. The transition from B-DNA to single-stranded DNA (ssDNA) is called DNA melting, and it is necessary for many fundamental processes such as DNA replication, gene transcription, and DNA damage repair. In vivo, DNA melting can occur with assistance from DNA helicases or ssDNA binding proteins (1, 2). In vitro, DNA melting can occur by directly heating or pulling the two complementary strands apart in a single-molecule unzipping experiment (3).

Double-stranded DNA can exist in several different structures from the B-form, such as A-DNA and Z-DNA. These alternative structures can be promoted under certain conditions (4, 5). dsDNA can also exist in elongated forms in the presence of DNA damage repair proteins, such as RecA and Rad51 (6), or DNA intercalating ligands, such as the dyes YOYO-1 and ethidium bromide (7). Mechanical stretching of DNA may produce a similar transition.

A structural transition, referred to as the DNA overstretching transition, occurs at a force of around 65 pN. After this transition, DNA is stretched to about 1.7 times the contour length pertaining to the B-form (8, 9). Since its discovery in 1996 there has been a debate about the mechanism of this transition and the nature of overstretched DNA. The central question is whether overstretched DNA is (*i*) ssDNA due to force-induced melting of the duplex, or (*ii*) a unique elongated form of dsDNA (S-DNA) resulting from a hypothetical B-to-S transition (8, 9).

Both models have strengths and weaknesses in the interpretation of experimental data. A series of experiments support force-induced melting that leads to one ssDNA strand under tension through peeling from nicks or open ends of DNA or two separated single strands under tension through melting inside the DNA (internal melting) (10–15). Particularly, studies of the dependence of the transition force on temperature $F_{ov}(T)$ have determined ΔS and ΔH during the transition in dye-free conditions (14). The values are in good agreement with the thermal melting transition (16), and they disfavor a nonmelting mechanism. Whether the overstretched DNA has only one strand or two strands under tension can be studied by the dependence of the transition force on the ionic strength (15). Two such experiments have been reported. One study supports one strand (15), and the other study supports two strands under tension (10). Thus, based on these experiments, peeling and melting have been proposed to explain the DNA overstretching transition. Furthermore, force-induced DNA melting was also reported in full-atom molecular dynamics simulations (17).

In contrast, observations in a different series of experiments imply a nonmelting mechanism. In Experiment 1, the force-response of overstretched DNA is inconsistent with that of one ssDNA strand or two noninteracting ssDNA strands (18, 19). In Experiment 2, a second transition at an even higher force has frequently been observed that leads to final strand separation after the 65-pN overstretching transition (19–22). The existence of this second transition, which is definitely a melting transition, supports the notion that the first transition (at approximately 65 pN) is not a melting transition (19–21). In Experiment 3, Paik, et al., and some of us, showed that end-blocked, torsion-unconstrained DNA (which prevents peeling) still undergoes a nonhysteretic DNA overstretching transition at approximately 65 pN (19, 23). A DNA melting mechanism, however, may also explain these experimental results. For example, the unique force-response in Experiment 1 may represent an internally melted DNA whose two strands are interacting with each other. The secondary transition in Experiment 2 may be explained by breaking the last base pairs holding the strands together due to the heterogeneity in the DNA sequence (24). The nonhysteretic transition

in Experiment 3 on the end-blocked, torsion-unconstrained DNA may be an internal DNA melting transition. In addition, simulations and theoretical modeling studies suggest the existence of nonmelted elongated dsDNA (25, 26).

Theoretically, these two conflicting mechanisms can be reconciled by the existence of two modes of DNA overstretching transitions at approximately the same force and elongation (18), which may be the origin of confusion in the field. Consistent with this view, a series of experiments by our lab have revealed a hysteretic transition and a nonhysteretic transition at approximately 65 pN, which can be selected or coexist via small changes in factors that affect DNA base pair stability (20). The hysteretic transition has been shown to be a peeling transition. Whether the nonhysteretic transition leads to a previously proposed nonmelted "S-DNA" (8, 9, 18) or an internally melted DNA (10, 15) remains unclear. Due to this uncertainty, hereafter we refer the DNA after the nonhysteretic transition as "nonhysteretic overstretched DNA."

This research aims to provide new insights to the understanding of the following two major questions about DNA overstretching transitions: (*i*) whether "nonhysteretic overstretched DNA" is internally melted DNA, and (*ii*) how the selection between the hysteretic peeling transition and the nonhysteretic overstretching transition depends on experimental conditions. Crucial to the success of this research, an unambiguous experimental indicator is needed to judge whether the transitions are related to DNA melting. One possible approach is to stain the overstretched DNA with fluorescence dyes specific to ssDNA or dsDNA in order to visualize the DNA structural compositions directly (12). This approach, however, has a disadvantage of perturbing the stability of DNA structures, and it may influence the experimental outcomes. Therefore, to eliminate possible effects of DNA binding agents, it is important to study overstretching based on the intrinsic properties of the transitions and resulting structures of

naked DNA. One intrinsic property is the thermodynamics of the transitions. ΔS and ΔH during DNA melting have been studied extensively and are well characterized (16). If the nonhysteretic overstretching transition is not a DNA melting transition, these values are expected to differ from the values pertaining to DNA melting. In addition, intrinsic structural properties of an overstretched DNA, such as the number (one or two) of strands under tension. In the case of two strands, their spatial proximity may provide further important insights. In this contribution, these intrinsic properties are carefully examined for the hysteretic peeling transition and the nonhysteretic overstretching transition without using any DNA binding dyes.

As pointed out by Rouzina, et al. (15, 27), ΔS and ΔH during DNA overstretching transition can be directly determined by measurements of $F_{ov}(T)$ using the following equations: $\Delta S = -(\partial F_{ov}/\partial T)\Delta b$ and $\Delta G = \Delta\Phi + \Delta H - T\Delta S = 0$. Here Δb is the DNA extension change per base pair during the transition (*SI Appendix, Extension changes during transition*), $\Delta\Phi$ is the force dependent free energy change that can be calculated with force-responses of B-DNA and overstretched DNA (*SI Appendix, Entropy and enthalpy changes*). According to recent studies from our lab, there exist two distinct transitions based on whether hysteresis exists (19, 20). Previous measurements of ΔS and ΔH, however, do not demonstrate any apparent distinct values (14). One possibility is that the hysteretic and nonhysteretic transitions are DNA melting transition giving similar values of ΔS and ΔH. An alternative possibility is that the hysteretic and the nonhysteretic transitions have distinct values of ΔS and ΔH. Under those experimental conditions, however, DNA only underwent the peeling transition; thus, the other transition type was not observed. To test these possibilities, we remeasured $F_{ov}(T)$ them over a wider temperature range and determined ΔS and ΔH during respective transitions.
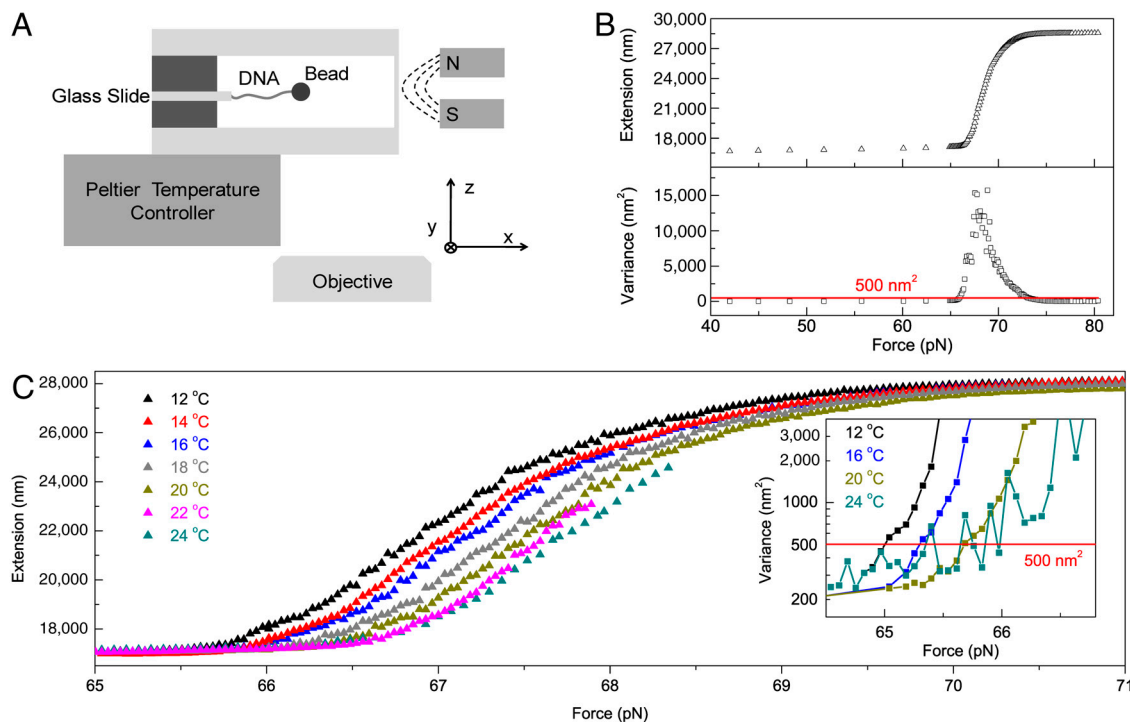
Fig. 1. Determination of F_{ov}. (*A*) Schematic diagram of the transverse magnetic tweezers. A peltier chip was used to control the temperature. See *SI Appendix, Magnetic tweezers measurements* and *SI Appendix, Temperature control and measurement* for details. (*B*) DNA overstretching transition in the nonhysteretic transition represented by force-extension (top) and force-variance (bottom) curves measured at 15 °C in 500 mM NaCl (pH 7.5). The threshold value of variance approximately 500 nm² (red line) in the force-variance curve was used to determine the onset of the transition (*SI Appendix, Determination of the transition force*). (*C*) DNA overstretching transition in the pure nonhysteretic transition (12–20 °C) and in the transition that contains hysteretic transition (22–24 °C). Inset shows the force-variance curves for four temperatures close to the onset of the transition, the red line corresponds to variance approximately 500 nm².

In addition to the measurements of $F_{ov}(T)$, important hints to possible structures of an overstretched DNA can be obtained by studying F_{ov} as a function of ionic strength $F_{ov}(I/I_0)$ (15). Here I is ionic strength, which is also the concentration of NaCl in this research, and $I_0 = 1$ M, the standard ionic strength. From $F_{ov}(I/I_0)$, a linear relation as a function of $\ln(I/I_0)$ exists with a slope $\partial F_{ov}/\partial \ln(I/I_0) = \nu(k_B T/l_B)$ for $I \ll I_0$. $l_B \sim 0.71$ nm is the Bjerrum length in water at room temperature. The structural coefficient ν is approximately 1.2 if the transition leads to one strand under tension while the other recoils (i.e., peeling), and ν is approximately 0.5 if the two strands are tightly associated with an interstrand distance considerably less than the Debye screening length. In this research, we also remeasured $F_{ov}(I/I_0)$ to see whether there exist distinct values of ν during the respective two transitions. Finally, phase diagrams for the selection of transitions are constructed from these results.

Results

Our results were based on measurements of $F_{ov}(T)$ and $F_{ov}(I/I_0)$ using a transverse magnetic tweezers setup (28) (Fig. 1A, *SI Appendix, Magnetic tweezers measurements*, and *SI Appendix, Temperature control and measurement*). In our experiments, F_{ov} is determined at the onset of the transition (Fig. 1 B and C) in order to attribute the force to a specific transition (*SI Appendix, Determination of transition types*). Analogous to other phase transitions, a clear signature at the onset of the overstretching transition is a dramatic increase in extension fluctuations. In our experiments, F_{ov} is defined as the force where the variance of the DNA extension increased to 500 nm².

To find the onset transition, cycling between a force below the transition force and a series of increasing higher forces are performed (*SI Appendix*, Fig. S4). At each of the higher forces, the DNA is held for 10 s (Figs. 1–4), during which the DNA extension and variance are measured. The force-extension and force-variance curves in Fig. 1 B and C were obtained by this method. If a variance of greater than 500 nm² is found, the corresponding force is identified as F_{ov}. In addition to determining F_{ov}, force cycling allows us to determine the transition types. In the peeling transition, hysteresis in extension change will be observed due to the slow reannealing process that occurs at the lower forces; whereas, in the nonhysteretic transition, no hysteresis in extension change will be observed due to much faster transition kinetics (19, 20, 29).

Fig. 1C inset shows that the variance monotonically increases as force increases in the nonhysteretic transition but not in the hysteretic peeling transition. This difference is caused by the slow stochastic nature of the peeling transition (19, 20, 29). Thus, determination of the transition force will have a larger variation in the hysteretic peeling transition than it will have in the nonhysteretic transition (*SI Appendix*, Fig. S6).

Using the above method, F_{ov} was determined at different temperatures from which ΔS and ΔH could be calculated. Fig. 2A shows $F_{ov}(T)$ measured in 150 mM NaCl and pH 7.5. A piecewise linear temperature response was revealed with two distinct slopes: $\partial F_{ov}/\partial T \sim 0.12$ pN/K from 11 °C to 18 °C, where the nonhysteretic transition was determined, and $\partial F_{ov}/\partial T \sim -0.77$ pN/K at T greater than 18 °C, where the hysteretic peeling transition was determined. Switching from nonhysteretic transition to hysteretic peeling transition as temperature increases is consistent with an earlier observation that the level of hysteresis can be suppressed by lowering temperature (30). We emphasize that the approximately 18 °C switching temperature (temperature at which the transition switches from the nonhysteretic transition to the hysteretic peeling transition) observed here is likely a response of the less stable AT-rich DNA region (*SI Appendix, Determination of the transition force*).

Fig. 2B shows another two independent experiments performed in 10 mM (blue) and 500 mM (red) NaCl. In 10 mM
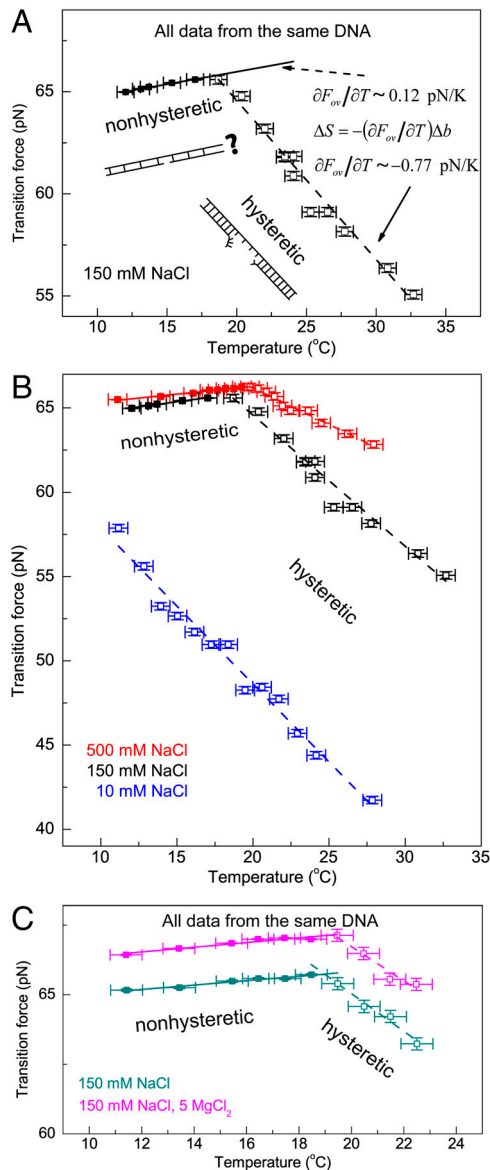
Fig. 2. Measurements of $F_{ov}(T)$ including error bars in both force (*SI Appendix*, Fig. S6) and temperature (*SI Appendix*, Fig. S2D). In the nonhysteretic transition, F_{ov} is denoted by colored filled squares and fitted to a linear function (solid line). In the hysteretic transition, F_{ov} is denoted by colored open squares, and it is fitted to a linear function (dashed line). (A) $F_{ov}(T)$ in 150 mM NaCl and pH 7.5 (black). A linear relation with a slope of approximately 0.12 pN/K was determined in the nonhysteretic transition ($T < 18$ °C). The slope remains unchanged if the midpoint or the terminus of the transition was used to determine the transition force (*SI Appendix, Determination of the transition force*). A different linear relation with a slope of -0.77 pN/K was determined in the hysteretic transition ($T > 18$ °C). The hysteretic transition has been agreed to be peeling of one strand from the other, while the nonhysteretic transition leads to an undetermined DNA structure, which are illustrated in the panel. (B) In 500 mM NaCl (red), a similar piecewise linear relation was obtained with a slope of approximately 0.10 pN/K in the nonhysteretic transition and approximately -0.44 pN/K in the hysteretic transition. In 10 mM NaCl (blue), only the hysteretic transition occurred and a single linear region was observed with a slope of approximately -0.92 pN/K. The data obtained in 150 mM (Fig. 2A) are also plotted for comparison (black). More independent experiments obtained from other DNA molecules are shown in *SI Appendix*, Fig. S8. (C) The effects of Mg^{2+} to DNA overstretching in 150 mM NaCl and pH 7.5. Without Mg^{2+} (dark cyan), switching from the nonhysteretic transition with a slope of approximately 0.08 pN/K to the hysteretic transition with a slope of approximately -0.68 pN/K occurred at approximately 18.5 °C. In the presence of 5 mM Mg^{2+} (magenta), switching from the nonhysteretic transition with a slope of approximately 0.08 pN/K to the hysteretic transition with a slope of approximately -0.62 pN/K occurred at approximately 19.4 °C.

Table 1. Comparison of ΔS and ΔH between our results and that reported in thermal melting experiments

Quantities	Our data, nonhysteretic transition		Our data, hysteretic transition			Santa Lucia (16), thermal melting		
I mM	150	500	10	150	500	10	150	500
ΔS cal/(K.mol)	-3.8 ± 0.6	-3.0 ± 0.7	26.4	21.2 ± 3.5	14.2 ± 1.6	24.7	23.2	22.5
ΔH kcal/mol	0.9 ± 0.2	1.1 ± 0.2	8.6	7.7 ± 1.6	5.5 ± 1.0	8.2	8.2	8.2

NaCl, the transition was entirely the hysteretic peeling transition in the experimental temperature range with a slope of approximately -0.92 pN/K; whereas, in 500 mM NaCl, a piecewise linear temperature response similar to that in Fig. 2A was observed with a slope of approximately 0.10 pN/K in the nonhysteretic transition and approximately -0.44 pN/K in the hysteretic peeling transition. To better extrapolate these results to in vivo conditions, where magnesium exists in a mM concentration range, we also studied the effects of magnesium. In 150 mM NaCl, Fig. 2C shows that the piecewise linear temperature response still exists in 5 mM MgCl$_2$, with similar slopes to the experimental data obtained in the absence of magnesium for the same DNA. The apparent effects of magnesium are that: it increases $F_{ov}(T)$ by approximately 1.5 pN, which is in agreement with previous studies (31), and it increases the switching temperature by less than 1 °C.

Multiple independent experiments (*SI Appendix*, Fig. S8) have yielded the average and standard deviation of the slopes of 0.10 ± 0.02 pN/K in 500 mM NaCl (ten experiments) and 0.12 ± 0.02 pN/K in 150 mM NaCl (six experiments) in the nonhysteretic transition; approximately -0.45 ± 0.05 pN/K in 500 mM NaCl (three experiments), and approximately -0.67 ± 0.11 pN/K in 150 mM NaCl (five experiments) in the hysteretic peeling transition. These slopes allowed us to calculate ΔS and ΔH per base pair during the nonhysteretic transition and the hysteretic peeling transition (*SI Appendix, Entropy and enthalpy changes*) and compare them with that determined in the thermal melting transition (averaged over a sequence with 50% GC content) (16) shown in Table 1.

It is of interest to know whether the two strands of DNA are in close proximity to each other after the two respective transitions.
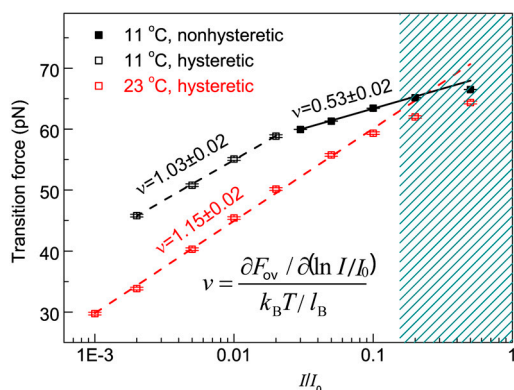

Fig. 3. Measurements of $F_{ov}(I/I_0)$ at two temperatures: 11 °C (open black squares for the hysteretic transition and filled black squares for the nonhysteretic transition) and 23 °C (red squares for the hysteretic transition). At 11 °C, a piecewise linear function of $\ln(I/I_0)$ was observed separated by a switching ionic strength of approximately 20 mM NaCl. It is characterized by a smaller slope of 2.9 ± 0.1 pN (black solid line) in the nonhysteretic transition and a larger slope of 5.7 ± 0.1 pN (black dashed line) in the hysteretic transition. At 23 °C, only the hysteretic transition was observed. A single linear region with a slope of 6.6 ± 0.1 pN (red dashed line) was observed. From these slopes ν was calculated. The lines shown in the figure are linear fits in the respective transitions up to $I \sim 100$ mM excluding the shadowed area where the theory is not applicable. Note: the standard deviation in force is plotted as error bars in the figure, which are similar to the symbol size so they are not apparent in the figure.

Therefore, we studied $F_{ov}(I/I_0)$. Fig. 3 shows two independent experiments at 11 °C (black) and 23 °C (red). At 11 °C, F_{ov} was found to be a piecewise linear function of $\ln(I/I_0)$, with two distinct slopes: 2.9 ± 0.1 pN in greater than 20 mM NaCl, where the nonhysteretic transition was determined, and 5.7 ± 0.1 pN in less than 20 mM NaCl where the hysteretic peeling transition was determined. These slopes correspond to $\nu = 0.53 \pm 0.02$ in the former and $\nu = 1.03 \pm 0.02$ in the latter. According to the predictions by Rouzina, et al. (15), $\nu = 0.53 \pm 0.02$ infers that the interdistance between the strands of the overstretched DNA is less than one Debye length (approximately 1 nm at 100 mM NaCl). This result suggests that the two strands of the "nonhysteretic overstretched DNA" are likely in close proximity. Moreover, $\nu = 1.03 \pm 0.02$ observed in the hysteretic peeling transition is close to the theoretically predicted value of 1.2 for the hysteretic peeling transition (15). In another experiment at 23 °C, the transition was determined to be the hysteretic peeling transition for 1 mM $< I <$ 500 mM. The corresponding slope is 6.6 ± 0.16 pN and $\nu = 1.15 \pm 0.02$. As shown in Fig. 3, the linear range is only up to 100 mM; therefore, our fittings are up to 100 mM NaCl-the same range as that used by Wenner, et al. (10).

Based on the experimentally determined force responses of the respective DNA states (B-DNA, ssDNA, or "nonhysteretic overstretched DNA") (*SI Appendix, Extension changes during transition*), ΔS and ΔH during the DNA melting transition obtained in previous DNA thermal melting transition (16), and ΔS and ΔH during the nonhysteretic transition measured in this research (Table 1), as well as $F_{ov}(I/I_0)$ measured in this research (Fig. 3), we can construct phase diagrams to predict the states of a DNA molecule with open ends or nicks and the selection of the transitions as a function of external force F, temperature T and ionic strength I (details in *SI Appendix, Phase diagrams*).

For clarity, we first consider the phase diagram projected onto the F-T plane for a fixed ionic strength of 150 mM. The boundary between the B-DNA and ssDNA (solid colored lines) where the free energy change $\Delta G^{\text{B-ss}}(F, T) = 0$ can be calculated from existing entropy and enthalpy data obtained from DNA thermal melting experiments (16). This boundary will vary with GC content. Because there is no existing free energy data of the nonhysteretic transition, and our prior studies have shown that the nonhysteretic transition is insensitive to GC content (19, 20), we used the entropy and enthalpy changes in Table 1 to calculate the boundary by $\Delta G^{\text{B-NHO}}(F, T) = 0$, where NHO refers to "nonhysteretic overstretched" for short. The boundary between "nonhysteretic overstretched DNA" and ssDNA (dashed line) is calculated by $\Delta G^{\text{NHO-ss}}(F, T) = \Delta G^{\text{B-ss}}(F, T) - \Delta G^{\text{B-NHO}}(F, T) = 0$. These three lines then determine the phase boundaries of the system and meet at a triple point that corresponds to the switching temperature that was previously introduced. The data obtained from studies of $F_{ov}(T)$ in Fig. 2 A and C are replotted in Fig. 4A for comparison.

We have mentioned that the selection of the transitions depends on factors that affect DNA base pair stability. Analogous to the phase diagram, we can construct a phase diagram for the selection of the transitions. For a given GC content, the point at which the change from a nonhysteretic transition to a hysteretic peeling transition is given by the switching temperature or triple point. Using similar calculations as above, we can calculate a line in the I-T plane that divides these two transitions. Each line in
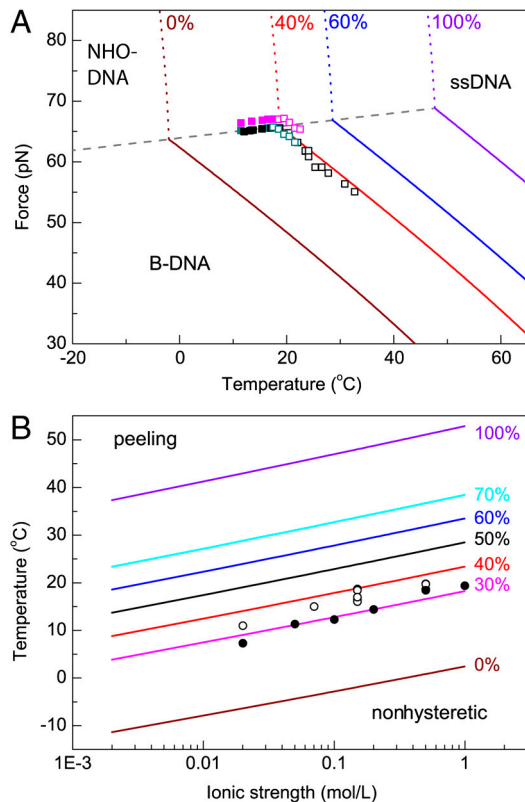
Fig. 4. Phase diagrams for states and transitions. (*A*) The phase diagram of B-DNA, ssDNA, and the nonhysteretic overstretched DNA (referred as NHO-DNA in the figure) projected onto the *F-T* plane in 150 mM NaCl. For each GC percentage, the solid line is the boundary between B-DNA and ssDNA and the dotted line is the boundary between the nonhysteretic overstretched DNA and ssDNA. The point where the two boundaries meet is the triple point. The gray dashed line to the left of the triple point is the boundary between B-DNA and the nonhysteretic overstretched DNA. The data from Fig. 2 *A* and *C* are plotted together in the same symbols for comparison. (*B*) The selection of the transitions as a function of ionic strength, temperature, and sequence. Predicted phase boundaries for different GC contents are shown in different colors. In the region above a line, the transition will be via hysteretic peeling transition, and the region below, a nonhysteretic transition will occur. Experimental data of the dependence of the switching temperature on ionic strength from the same DNA molecule (filled circles) and from other ten DNA molecules (open circles) are also plotted for comparison.

Fig. 4*B* corresponds to a different GC percentage, and it divides the *I-T* plane into the hysteretic peeling transition region (above of the line) and the nonhysteretic transition region (below the line). The triple points obtain from different experiments are plotted in Fig. 4*B* for comparison. The filled circles obtained on the same DNA, while open circles are obtained from ten other different DNA molecules. Fig. 4 helps to emphasize that the experimentally observed transition is sensitive to temperature, ionic strength and GC content.

Discussion

We have shown that $F_{ov}(T)$ and $F_{ov}(I/I_0)$ have distinct trends in the nonhysteretic transition and the hysteretic peeling transition. ΔS and ΔH determined in the hysteretic peeling transition are consistent with those measured in DNA thermal melting transition experiments (16). The slight difference between our data and those from DNA thermal melting could be explained by a finite heat capacity change during DNA melting (*SI Appendix, Effects of heat capacity change*) (14, 15).

Striking results were found in the nonhysteretic transition. ΔS is a small negative value, which may suggest an ordered "nonhysteretic overstretched DNA" structure that has slightly lower

entropy than B-DNA together with surrounding water and ion distributions. The small ΔH value of approximately 1 kcal/mol is about one order of magnitude smaller than that measured in thermal melting or hysteretic peeling transition. In addition, our study of $F_{ov}(I/I_0)$ was consistent with a picture that the two strands in the nonhysteretic overstretched DNA are close to each other at an interstrand distance within the Debye screening length (15).

One important question remains regarding the exact structure of the nonhysteretic overstretched DNA. We considered two possibilities: (*i*) the structure could be some new regular double-stranded structure with regular short-ranged bonds and residual helicity (i.e., the previously proposed "S-DNA"), or (*ii*) the structure could be the two separated strands with broken hydrogen bonds. These two melted strands, however, can still interact with each other strongly via electrostatic and steric interactions. We cannot draw a firm conclusion between these two possibilities because ΔS and ΔH during the force-induced DNA internal melting transition were not directly measured.

Providing the final answer regarding the structure of the nonhysteretic overstretched DNA is not the purpose of this research. The main point of this research was to show that there exist two transitions that have distinct entropy and enthalpy changes during overstretching of DNA with open ends or nicks; however, it is interesting to note these results can be explained by the existence of a nonmelting DNA overstretching transition, which warrants further study. It is also worthwhile to mention a few previous experiments that may be related to this research. It has been found that torsion-constrained DNA did not undergo overstretching transition at approximately 65 pN unless the DNA is underwound (12). This result is also consistent with results obtained from another single-DNA stretching experiment by Bryant, et al. (32), and it is consistent with the high resolution atomic force microscopy imaging of DNA overstretched by molecular combing method (33).

These results raise interesting questions regarding the physiological relevance of the DNA overstretching transition. The hysteretic peeling transition is sensitive to factors that affect DNA base pair stability, and the transition force can be as low as 40 pN in 150 mM NaCl for AT-rich DNA at 37 °C (Fig. 4*A*). This force is close to the force range that can be generated by a single RNA polymerase (34) or DNA polymerase (35) in the force range of 20–40 pN. In comparison, the nonhysteretic transition is much less sensitive to factors that affect base pair stability. According to the predictions in Fig. 4*B*, the nonhysteretic transition may occur at greater than 25 °C for GC-rich DNA. The approximately 60 pN transition force is about 30 pN greater than the reported force range that can be generated by RNA polymerase (34) or DNA polymerase (35). In the presence of DNA intercalators, however, it is known that elongation of double DNA requires less force. For example, recent experiments showed that the presence of a YOYO-1 force of a few picoNewtons could elongate DNA contour by approximately 1.5-fold (36). Although the structure of the nonhysteretic overstretched DNA remains unknown, we imagine that DNA bound with YOYO-1 may resemble the DNA structure because it is only 10% shorter. In cells, DNA-distorting proteins play important roles in processing information in DNA and in organizing chromosome DNA. Among these proteins, many of them use side chain intercalation to distort the DNA backbone (37). Therefore, binding of these proteins may also be susceptible to DNA tension.

Materials and Methods

Refer to *SI Appendix* for details of the DNA construct, magnetic tweezers measurements, temperature control and measurement, determination of transition types, determination of the transition force, extension changes during transition, entropy and enthalpy changes, phase diagrams, elimination of thermal expansion effects, convection in the flow channel, and effects of heat capacity change.

1. Caruthers JM, McKay DB (2002) Helicase structure and mechanism. *Curr Opin Struct Biol* 12:123–133.
2. Iftode C, Daniely Y, Borowiec JA (1999) Replication protein A (RPA): the eukaryotic SSB. *Crit Rev Biochem Mol* 34:141–180.
3. Essevaz-Roulet B, Bockelmann U, Heslot F (1997) Mechanical separation of the complementary strands of DNA. *Proc Natl Acad Sci USA* 94:11935–11940.
4. Franklin RE, Gosling RG (1953) Molecular configuration in sodium thymonucleate. *Nature* 171:740–741.
5. Wang AHJ, et al. (1979) Molecular-structure of a left-handed double helical DNA fragment at atomic resolution. *Nature* 282:680–686.
6. Kowalczykowski SC, Eggleston AK (1994) Homologous pairing and DNA strand-exchange proteins. *Annu Rev Biochem* 63:991–1043.
7. Sischka A, et al. (2005) Molecular mechanisms and kinetics between DNA and DNA binding ligands. *Biophy J* 88:404–411.
8. Smith SB, Cui Y, Bustamante C (1996) Overstretching B-DNA: the elastic response of individual double-stranded and single-stranded DNA molecules. *Science* 271:795–799.
9. Cluzel P, et al. (1996) DNA: an extensible molecule. *Science* 271:792–794.
10. Wenner JR, Williams MC, Rouzina I, Bloomfield VA (2002) Salt dependence of the elasticity and overstretching transition of single DNA molecules. *Biophys J* 82:3160–3169.
11. Williams MC, Wenner JR, Rouzina I, Bloomfield VA (2001) Effect of pH on the overstretching transition of double-stranded DNA: evidence for force-induced DNA melting. *Biophys J* 80:874–881.
12. van Mameren J, et al. (2009) Unraveling the structure of DNA during overstretching by using multicolor, single-molecule fluorescence imaging. *Proc Natl Acad Sci USA* 106:18231–18236.
13. Shokri L, McCauley MJ, Rouzina I, Williams MC (2008) DNA overstretching in the presence of glyoxal: structural evidence of force-induced DNA melting. *Biophys J* 95:1248–1255.
14. Williams MC, Wenner JR, Rouzina I, Bloomfield VA (2001) Entropy and heat capacity of DNA melting from temperature dependence of single molecule stretching. *Biophys J* 80:1932–1939.
15. Rouzina I, Bloomfield VA (2001) Force-induced melting of the DNA double helix. 2. Effect of solution conditions. *Biophys J* 80:894–900.
16. SantaLucia J, Jr (1998) A unified view of polymer, dumbbell, and oligonucleotide DNA nearest-neighbor thermodynamics. *Proc Natl Acad Sci USA* 95:1460–1465.
17. Santosh M, Maiti PK (2009) Force induced DNA melting. *J Phys-Condens Mat* 21:034113.
18. Cocco S, Yan J, Leger JF, Chatenay D, Marko JF (2004) Overstretching and force-driven strand separation of double-helix DNA. *Phys Rev E* 70:011910.
19. Fu H, et al. (2011) Transition dynamics and selection of the distinct S-DNA and strand unpeeling modes of double helix overstretching. *Nucleic Acids Res* 39:3473–3481.
20. Fu H, Chen H, Marko JF, Yan J (2010) Two distinct overstretched DNA states. *Nucleic Acids Res* 38:5594–5600.
21. Rief M, Clausen-Schaumann H, Gaub HE (1999) Sequence-dependent mechanics of single DNA molecules. *Nat Struct Biol* 6:346–349.
22. Danilowicz C, et al. (2009) The structure of DNA overstretched from the 5′5′ ends differs from the structure of DNA overstretched from the 3′3′ ends. *Proc Natl Acad Sci USA* 106:13196–13201.
23. Paik DH, Perkins TT (2011) Overstretching DNA at 65 pN does not require peeling from free ends or nicks. *J Am Chem Soc* 133:3219–3221.
24. Williams MC, Rouzina I, McCauley MJ (2009) Peeling back the mystery of DNA overstretching. *Proc Natl Acad Sci USA* 106:18047–18048.
25. Lebrun A, Lavery R (1996) Modelling extreme stretching of DNA. *Nucleic Acids Res* 24:2260–2267.
26. Haijun Z, Yang Z, Zhong-can O-Y (1999) Bending and base-stacking interactions in double-stranded DNA. *Phys Rev Lett* 82:4560–4563.
27. Rouzina I, Bloomfield VA (2001) Force-induced melting of the DNA double helix 1. Thermodynamic analysis. *Biophys J* 80:882–893.
28. Yan J, Skoko D, Marko JF (2004) Near-field-magnetic-tweezer manipulation of single DNA molecules. *Phys Rev E* 70:011905.
29. Gross P, et al. (2011) Quantifying how DNA stretches, melts and changes twist under tension. *Nat Phys* 7:731–736.
30. Mao H, Arias-Gonzalez JR, Smith SB, Tinoco I, Jr, Bustamante C (2005) Temperature control methods in a laser tweezers system. *Biophys J* 89:1308–1316.
31. Fu H, Chen H, Koh C, Lim C (2009) Effects of magnesium salt concentrations on B-DNA overstretching transition. *Eur Phys J E* 29:45–49.
32. Bryant Z, et al. (2003) Structural transitions and elasticity from torque measurements on DNA. *Nature* 424:338–341.
33. Maaloum M, Beker A-F, Muller P (2011) Secondary structure of double-stranded DNA under stretching: Elucidation of the stretched form. *Phys Rev E* 83:031903.
34. Davenport RJ, Wuite GJ, Landick R, Bustamante C (2000) Single-molecule study of transcriptional pausing and arrest by *E. coli* RNA polymerase. *Science* 287:2497–2500.
35. Wuite GJ, Smith SB, Young M, Keller D, Bustamante C (2000) Single-molecule studies of the effect of template tension on T7 DNA polymerase activity. *Nature* 404:103–106.
36. Gunther K, Mertig M, Seidel R (2010) Mechanical and structural properties of YOYO-1 complexed DNA. *Nucleic Acids Res* 38:6526–6532.
37. Werner MH, Gronenborn AM, Clore GM (1996) Intercalation DNA kinking, and the control of transcription. *Science* 271:778–784.